International Journal of Innovation and Applied Studies
ISSN 2028-9324 Vol. 44 No. 1 Nov. 2024, pp. 125-140

http://www.ijias.issr-journals.org/

Sizing of a hybrid energy production system

Bati Ernest Boya Bi, Ekoun Magloire Paul Koffi, Kamenan Blaise Koua, and Prosper Gbaha

Groupe Energies Nouvelles et renouvelables, Laboratoire de Mécanique et Sciences des Matériaux, URMI 18, Institut National Polytechnique Houphouët Boigny, B.P 1093, Yamoussoukro, Côte d'Ivoire

ABSTRACT: *Objective*: Since solar energy allows decentralized production of electricity, it can help solve the problem of electrifying isolated sites where a large number of individuals do not have access to energy. This work aims to size a multi-source system for optimal management of the energy produced.
Method: We used an energy management strategy that is an algorithm, which determines at each moment the sharing of power between the different components of the system.
Findings: The sizing tools allowed us to establish relationships between the powers of the components by simple rules, to define the solar power and the storage volume necessary to meet the demand of a load on a given site.
Novelty: This study allowed us to set up an electrical architecture and a control strategy capable of limiting conversion losses and optimizing energy management within the system.

KEYWORDS: sizing, hybrid system, management strategy, algorithm, electrical architecture.

1 INTRODUCTION

The rapid depletion of fossil fuels worldwide has led to the search for new energy sources including renewable energies. Among the many alternatives, photovoltaics has been considered promising to meet the growing demand for energy [1]. Photovoltaic energy sources are inexhaustible, the conversion processes are less polluting and their availability is free [1; 2]. For remote systems such as telecommunication relays in desert areas, satellite ground stations or isolated sites that are far from a conventional energy system, hybrid systems have been considered attractive and preferred alternative sources [2; 3]. The new technological solutions proposed by hybrid generators, even if they are very complex compared to current single-source solutions, present on the other hand an obvious interest, considerable by their incomparable flexibility, their operating flexibility and their really attractive cost price [4 – 9]. However, these solutions require a laborious sizing based on a thorough knowledge of the renewable energy deposit of the installation site upstream, a rigorous management of the electrical energy produced downstream and a know-how that only experience in energy systems engineering can provide. Thus, several authors have studied hybrid energy production systems in order to find the optimal design. They have introduced different forms of optimization to find the right size and reduce the costs of hybrid systems [3; 4; 10 – 16]. However, there is not enough information on the hybrid photovoltaic – hydrogen energy storage – battery (PV-SEH-Batteries) energy production system. The objective of our study is therefore to size a hybrid photovoltaic – hydrogen energy storage – battery (PV-SEH-Batteries) system and to propose an optimal management method for the energy it produces. The aim is to propose a technological solution that will make it possible to exploit renewable energy resources for the production of electrical energy.

2 Materials And Method

2.1 Materials

2.1.1 Architectures Of Hybrid Power Generation Systems

The electric generators of a hybrid power generation system can be connected in different configurations. Two configurations are essential among these hybrid power generation systems:

- DC bus architectures [16; 17];
- Mixed DC-AC bus architectures [4; 10 – 18].

The two-bus configuration (DC and AC) has higher performance compared to the single-bus configuration (DC) [19]. The implementation of the two-bus configuration is more complicated because of the parallel operation [19]. The inverter must be able to operate autonomously and non-autonomously by synchronizing the output voltages.

The hybrid system that is the subject of our study therefore has a DC bus configuration. Figure 2.1 shows the architecture of the system studied. It is a hybrid Photovoltaic system – Energy storage via Hydrogen – Batteries. This system includes a photovoltaic generator, an inverter, converters, a DC bus and an energy storage unit. The energy storage unit consists of:

- A lead-acid battery pack (A);
- An electrochemical generation and storage system (Fuel cell, Electrolyser) (B);
- A Hydrogen Energy Storage (SEH) Battery system (C).

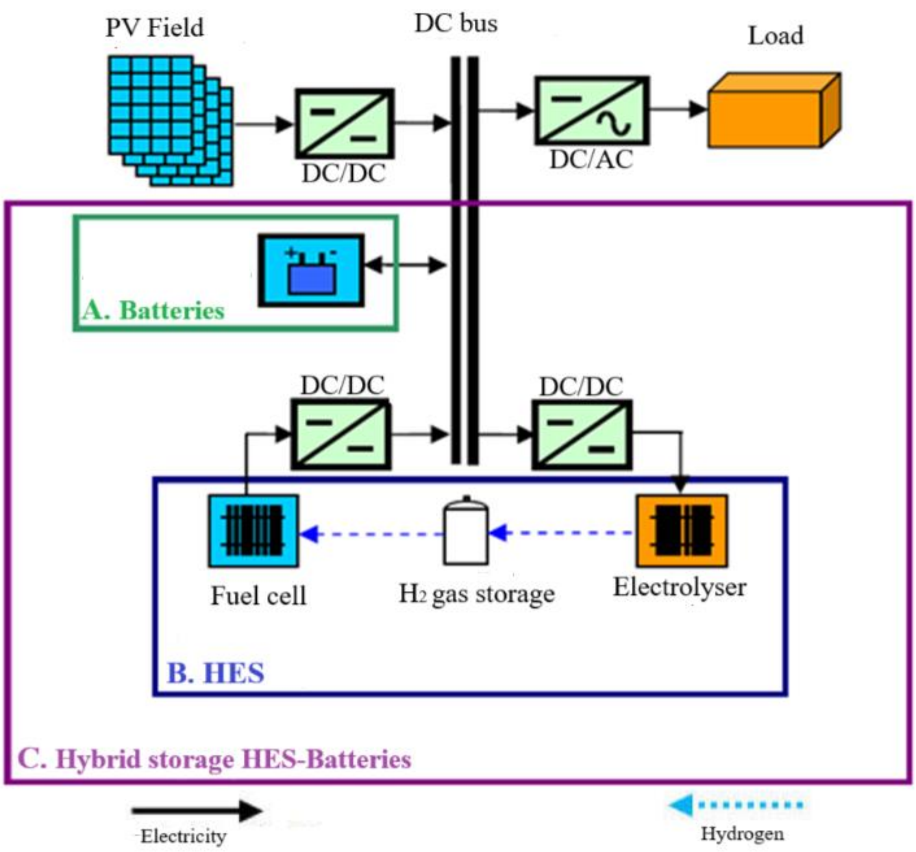

Fig. 1. Architecture of the system studied and the different types of storage

2.1.2 DESCRIPTION OF THE DIFFERENT ELEMENTS OF THE SYSTEM STUDIED

2.1.2.1 PHOTOVOLTAIC GENERATOR

Mainly composed of a photovoltaic (PV) field coupled to a DC/DC converter, the photovoltaic generator is the main source of energy production. It results from the association of PV modules mounted in series and in parallel. The energy generated by the PV system is affected by solar irradiation, temperature and cell type [10; 20].

2.1.2.2 CONVERTERS

The role of converters is to balance the energy flow between DC and AC elements.

For this purpose, three types of converters are often encountered in hybrid energy production systems, namely [21]:

- AC/DC rectifiers: These are simple devices with good efficiency and low cost, which are often used to charge batteries from an AC source;
- DC/AC inverters: They can operate autonomously to power AC loads or in parallel with AC sources. Inverters are autonomous when they impose their own frequency on the load. The non-autonomous inverter requires the presence of an AC source to operate;
- DC/DC choppers are used to adapt the voltage between two different sources.

2.1.2.3 ENERGY STORAGE UNIT

Energy storage is often used in hybrid energy production systems in order to be able to power the load for a relatively long period (hours or even months). The storage system also makes it possible to store energy in the event of excess production and to compensate for any temporary energy or power deficits during consumption peaks [22].

2.1.2.4 BATTERIES

Most of the batteries used in hybrid power generation systems are lead-acid [17]. Choosing the appropriate size of the battery pack requires an inclusive analysis of the battery charge and discharge requirements [17].

In our case, this pack is directly connected to the DC bus and imposes its voltage on it. Four 12-volt batteries are connected in series to have an open-circuit voltage of 48 volts. In operation, this voltage varies between 44 and 56 volts.

2.1.2.5 FUEL CELLS

A promising technology for efficient and clean electricity production [23], the fuel cell directly converts chemical energy into electrical energy. Its operating principle is quite simple and based on the reverse process of electrolysis [24].

The Proton Exchange Membrane (PEM) technology fuel cell with a lifespan of more than 30,000 hours in operation was used in this study [23], due to its simple peripheral and easy evacuation of the water produced.

In the case of using the SEH as sole storage, the presence of a very low capacity battery pack ensures the maintenance of the DC bus voltage.

2.1.2.6 ELECTROLYZER

An alkaline electrolyzer was used for our study because it has very good performance at the cell level (potential efficiency: 80%, faradaic efficiency: 99%) but has a complex peripheral that induces high intrinsic consumption. However, optimizing its peripheral will allow us to obtain the best overall efficiencies. We will use a high-pressure electrolyzer to avoid the use of an energy-consuming compressor in order to reduce the size of the gas storage unit [25].

2.2 SYSTEM SIZING METHOD

The hybridization of a power generation system allows to smooth the power delivered by the energy source and the bearing for a limited period, a partial or total unavailability of the energy source. The design of a hybrid power generation system requires the selection and sizing of the most appropriate combination of energy sources, converters and the storage system, as well as the implementation of an effective management strategy [26]. Sizing software is therefore an essential tool for the analysis and comparison of the different possible combinations of sources used in hybrid power generation systems. The main factors of the sizing are [26]:

- The environmental conditions of the site such as irradiance, temperature, humidity and wind speed;
- The load profile.

For the sizing of the system components, the following parameters are defined:

- The peak power of the solar field;
- The nominal power of the electrolyser and fuel cell components;
- The nominal capacity of the battery storage;
- The gas storage volume.

Part of the system parameters is set by analyzing its operation and its components. The other part is determined by optimization routines (these are.m files written in Matlab language that are called by the simulator.mdl file) to complete the definition of the system in terms of sizing.

2.2.1 Sizing Assumptions For Storage Components

2.2.1.1 Electrolyzer System

The nominal power (P_{nomel}) of the electrolyzer system is set proportionally to the peak power of the solar field ($P_{PV\ peak}$), translated by the following relationship [27]:

$$P_{nomel} = K_{el} \times P_{PV\ peak} \quad (1)$$

K_{el}: dimensional coefficient of the electrolyser. This coefficient depends on the type of storage used.

2.2.1.2 Hydrogen Energy Storage (HES) Alone

If HES is the only means of storage, then the nominal power (P_{nomel}) must be equal to the maximum power that can be produced by the solar field for maximum production of dihydrogen [27 – 29].

2.2.1.3 Hybrid HES-Batteries Storage

In this case, the expressed needs in dihydrogen are lower due to the presence of batteries that provide part of the energy demand. There is therefore an interaction between the dimensional parameters K_{el} and C_{nom} (nominal capacity of the batteries) whose adequate values were determined following a sensitivity study [27; 29 – 32].

2.2.2 Sensitivity Study

This part studies the impact of the dimensional parameters K_{el} for the electrolyser and C_{nom} for the batteries on the performance and the results of the sizing of the PV-HES-Batteries system. The aim is to determine the values of the couple (K_{el}, C_{nom}) which allows to obtain better simulation results [4; 29].

The case studied here concerns the INP-HB Center of Yamoussoukro (Ivory Coast). A load profile corresponding to an unfavorable case was used. The daily variation amplitudes (60% of the daily average power) and seasonal variation (30% of the annual average power) are significant [29]. The daily phase shift is 8 hours compared to noon (higher consumption in the evening) and the seasonal phase shift is 30 days compared to January 1st.

According to the work of BOYA BI et al., (2020) and J. LABBE., (2006), the recommended values of these dimensional parameters are: K_{el} = 0.8 and C_{nom} = 1.

It is on these values that we will rely to size our system.

2.2.3 FUEL CELL SYSTEM

Regardless of the type of storage used, the nominal power of the fuel cell system is set so that it can ensure the supply of energy to the load. This nominal power of the fuel cell system is given by the following equation [27 – 29]:

$$P_{nomfc} = K_{fc} \times P_{\max load} \quad (2)$$

The coefficient K_{fc} is introduced to take into account the losses in the DC/DC and DC/AC converters. The observation of the converter efficiencies over a year of simulation made it possible to evaluate the value of K_{fc}. Thus, the value of Kfc obtained is K_{fc} = 1.1 [27 – 29].

2.2.4 BATTERY SYSTEM

The available capacity of the battery pack must be able to allow the hybrid system to be autonomous for a few days during the most unfavorable period. For a PV-Batteries system, this autonomy is set at four days [27 – 32]. For a PV-HES Batteries system, the number of days of autonomy is set at 1 [27 – 32].

2.2.5 CONVERTERS

Their nominal powers correspond to the nominal powers of the components to which they are connected.

2.2.6 PHOTOVOLTAIC (PV) FIELD SIZING

2.2.6.1 CASE OF PV-HES AND PV-HES-BATTERIES SYSTEMS

An optimization algorithm (dichotomy) determines the peak power of the PV field so that the energy initially present in the storage at the beginning of the simulation year is equal to that present at the end of the simulation, which reflects the energy autonomy of the system over the year of operation [29].

For PV-HES and PV-HES-Batteries systems, the observed energy variable is the quantity of dihydrogen in terms of the number of moles in the gas storage. This variable (quantity of dihydrogen) is first set at a high threshold and its variation in the storage must be globally zero over the year [27 – 29; 33]. This assumes that the peak power of the PV field must be determined so that the production of dihydrogen by the electrolyser over the year is equal to the consumption of the fuel cell [29]. The energy management algorithm ensures that the state of charge SOC of the batteries is between the minimum SOC_{min} and maximum SOC_{max} limits allowed for the PV-HES-Batteries system [3; 29; 34].

2.2.6.2 PV-BATTERIES SYSTEM

Here, the peak power of the installed PV field is calculated by optimization so that the state of charge of the battery system (SOC) does not exceed the minimum authorized limit (SOC_{min}).

The energy management algorithm ensures that the battery storage usage condition is respected ($SOC < SOC_{max}$) [3; 19; 29; 34]. This approach is explained by the fact that the batteries are used daily for storage.

2.2.7 SIZING THE GAS STORAGE VOLUME

This consists of calculating the total quantity of dihydrogen produced by the electrolyser and the total quantity of dihydrogen consumed by the fuel cell. The difference between these two quantities every month corresponds to the storage volume [29].

3 RESULTS AND DISCUSSION

3.1 PARAMETERS OF THE DIFFERENT COMPONENTS OF THE SYSTEM

The following tables present the different input parameters of the simulator for each component of the systems studied.

Tableau 1. Simulation time parameters

Parameter name	Value	Unit	Description
t_{max}	24×365	Hour	Duration of the simulation

Tableau 2. PV field parameters (PW1650 produced by PHOTOWATT)

Parameter	Value	Unit	Description
N_{PV}	32	No unit	Number of solar modules
P_{max}	165	W	Maximum power of a module
$\mu_{P_{max}}$	-0.0043	W. °C^{-1}	Coefficient of variation of module power with temperature
NOCT	47.1	°C	Operating temperature of solar modules under standard conditions
$P_{PV-peak}$	$N_{PV} \times P_{max}$	W	Installed peak power of the PV field

Tableau 3. Lead acid battery pack parameters (Battery type: PowerSafe, 12XP160 manufactured by ENERSYS, sealed lead acid battery)

Parameter	Value	Unit	Description
U_{Bat_nom}	12	V	Nominal voltage of a unit block
C_{nom}	140	Ah	Nominal capacity of a unit block
I_{nom}	14	A	Nominal discharge current
ns	4	No unit	Number of branches in series
np	A calculer	No unit	Number of branches in parallel (in the case of SEH-battery hybrid storage: 1 day of autonomy without sun).

Tableau 4. The different states of charge (SOC) of the battery pack [27; 29]

Parameter	Value	Unit	Description
$\boldsymbol{SOC_{min}}$	30	$\%\boldsymbol{C_{nom}}$	SOC Minimum allowed
$\boldsymbol{SOC_{max}}$	95	$\%\boldsymbol{C_{nom}}$	SOC Maximum allowed
$\boldsymbol{SOC_{min1}}$	50	$\%\boldsymbol{C_{nom}}$	SOC Minimum intermediate
$\boldsymbol{SOC_{max1}}$	90	$\%\boldsymbol{C_{nom}}$	SOC Maximum intermediate

Tableau 5. Electrolyzer parameters

Parameter	Value	Unit	Description
$P_{nom\_el°}$	3600	W	Initial nominal power
N_{cel_el}	16	No unit	Number of cells in series
A_{el}	300	cm^2	Cell surface area
V_{EL}	1,84	V	Voltage of an elementary cell of the electrolyser
J_{EL}	0,57	A.cm^{-2}	Current density of an elementary cell of the electrolyser
π_{el}	10	bar_{abs}	Operating pressure of the electrolyser
τ	0,45	m^3/h	Maximum rate of production of dihydrogen (H_2)

Tableau 6. Dimensional coefficient of the electrolyser

Parameter	Value	Unit	Description
P_{nom_el}	$K_{el} \times P_{crête_{PV}}$	W	Nominal power after dimensioning
With HES as the only storage			
K_{el}	1	No unit	Electrolyzer scaling factor
With HES-battery hybrid storage			
K_{el}	0.8	No unit	Electrolyzer scaling factor

Tableau 7. Operating power of the electrolyser

Parameter	Value	Unit	Description
$P_{\min\_el}$	$0.1 \times P_{nom\_el}$	W	Minimum authorized power
$P_{\max\_el}$	P_{nom_el}	W	Maximum authorized power

Tableau 8. Fuel cell parameters (NEXATM module manufactured by Ballard)

Parameter	Value	Unit	Description
$P_{nom\_fc°}$	1200	W	Initial nominal power
N_{cel_fc}	50	No unit	Number of cells in series
A_{fc}	100	cm^2	Cell surface area
V_{Pac}	0,83	V	Voltage of an elementary cell of the PAC
J_{Pac}	0,29	$A.cm^{-2}$	Current density of an elementary cell of the PAC
S_{H_2}	1,01	No unit	Stoichiometry of dihydrogen
S_{O_2}	1,01	No unit	Stoichiometry of dioxygen
$\pi_{fc\_H_2}$	3	bar_{abs}	Operating pressure on the hydrogen side of the fuel cell
$\pi_{fc\_O_2}$	3	bar_{abs}	Operating pressure on the oxygen side of the fuel cell
Nb_{fc}	3	No unit	Number of fuel cells started up according to the load to be supplied

Tableau 9. Fuel cell operating power

Parameter	Value	Unit	Description
$\boldsymbol{P_{\min\_fc}}$	0	W	Minimum power

Tableau 10. HES-battery hybrid storage

Parameter	Value	Unit	Description
$P_{\min\_el}$	$0.1 \times P_{nom\_el}$	W	Minimum authorized power
$P_{\max\_el}$	P_{nom_el}	W	Maximum authorized power

Tableau 11. Gas storage tank parameters

Parameter	Value	Unit	Description
V	5	m^3	Tank volume (value we have fixed)
P_0	101320	Pa	Atmospheric pressure under standard conditions
$P_{\min stock}$	3	bar_{abs}	Minimum pressure in the tank
$P_{\max stock}$	10	bar_{abs}	Maximum pressure in the tank
R	8.314	SI	Ideal gas constant

Tableau 12. Converter parameters

Parameter	Value	Unit	Description
$\eta_{10\_DC/DC}$	93	%	Efficiency at 10% of the nominal power of the DC/DC converter
$\eta_{100\_DC/DC}$	98	%	Efficiency at 100% of the nominal power of the DC/DC converter
P_{nom_DC/DC_PV}	P_{max_load}	W	Nominal power of the DC/DC converter of the PV field
P_{nom_DC/DC_EL}	P_{nom_el}	W	Nominal power of the DC/DC converter of the electrolyser
P_{nom_DC/DC_FC}	$1.1 \times P_{max\_load}$	W	Nominal power of the DC/DC converter of the fuel cell

Tableau 13. Inverter parameters

Parameter name	Value	Unit	Description
η_{10_ond}	86	%	Efficiency at 10% of the inverter's nominal power
η_{100_ond}	97	%	Efficiency at 100% of the inverter's nominal power
P_{nom_ond}	P_{max_load}	W	Inverter nominal power

3.2 Energy Management Algorithms

Various energy management scenarios can be proposed depending on the available energy sources, energy consumption and the state of charge of the batteries for 24 hours to ensure the proper execution of the algorithm [28; 29; 35; 36]. For our study, we used computer simulation software, namely Matlab®-Simulink version R2012a, which allows us to determine, at any time, the operation of the different elements constituting the energy production system.

3.2.1 Different Operating Modes Of The System

The hybrid energy production system studied is composed of a 5 kW PV field, a fuel cell with a power of 3.6 kW and a battery pack with a nominal capacity of 140 Ah per battery. The hybrid energy production system is designed to supply a load (DC or AC) and an electrolyser. It is considered that:

- The PV field is the main source;
- The battery pack is used as a source or a load depending on whether there is a production deficit or an overproduction of the PV field;
- The fuel cell is a backup source;
- The load is always connected;
- The electrolyser is an auxiliary load to dissipate the surplus production.

To simplify the study, we assume that each component has two states (active and inactive) depending on the periods of the day. Indeed, depending on the available energy sources, the energy consumption and the state of charge of the batteries, different operating scenarios of the system are observed. Tables 14 and 15 give the state of each component of the hybrid system.

Tableau 14. Status of each component constituting the hybrid system [27 – 29]

State		Active	Inactive
Main source	Photovoltaic field	On a sunny day	• During the night • During a cloudy day • In case of breakdown
Auxiliary sources	Batteries	• During the incapacity of the primary source, for example when : 1. The weather conditions are poor ; 2. Load demand exceeds production ; 3. In case of failure of the main source • When the state of charge is between 50 and 90%	• During normal operation of the main source (PV) • Load demand equal to or less than production (Pload ≤ PPV)
	Fuel cell	• During main sources incapacity, • Battery SOC below low threshold (SOCmin< 0,5)	
Main load	DC & AC	The load is always connected.	
Auxiliary loads	Battery	In case of excess energy and SOC is lower than low threshold	When SOC is above high threshold (SOC_{max}= 0,90).
	Electrolyser	In case of excess energy and SOC is higher than high threshold.	In case of energy shortage or demand is satisfied (P_{load} = P_{SP})

Tableau 15. Different operating scenarios of the hybrid system [27 – 29]

Case	Period	PV	Batteries	P_{Diff}	FC	SOC	EL	Description
1	On a sunny or cloudy day	Ok	Rest	P_{Diff}= 0	OFF	0,5< SOC< 0,9	OFF	$P_{load} = P_{PV}$
2		Ok	Dump (source)	P_{Diff}< 0				$P_{load} = P_{PV} + P_{Bat}$
3		×						$P_{load} = P_{Bat}$
4		Ok	Rest		ON	SOC< 0,5		$P_{load} = P_{PV} + P_{FC}$
5		×						$P_{load} = P_{FC}$
6		Ok	Loaded (load)	P_{Diff}> 0	OFF			P_{PV}- P_{load} = P_{Bat}
7		Ok	Rest			SOC> 0,9	ON	P_{PV}- P_{load} = P_{EL}
8	During the night	×	Dump	P_{Diff}< 0	OFF	0,5 < SOC< 0,9	OFF	$P_{load} = P_{Bat}$
					ON			$P_{load} = P_{Bat} + P_{FC}$
9		×	Rest		ON	SOC< 0,5	OFF	$P_{load} = P_{FC}$
Ok		Normal operation (active)						
×		Inactive						

3.3 SUPERVISION SYSTEM OF THE HYBRID ENERGY PRODUCTION SYSTEM

The energy management between the different components of the hybrid energy production system is ensured by a management technique based on deterministic rules. It is designed taking into account all the operating scenarios of this hybrid system studied. The flowchart in figure 2 gives the operating principle of the energy management strategy of the hybrid system. First, the parameters of the different subsystems and the climatic data (temperature, illumination) were initialized. Then, the total power P_{MS} produced by the main source (PV) and the demand of the load P_{load} evaluated at each moment were estimated, in order to calculate the power difference P_{Diff}.

$$P_{Diff} = P_{MS} - P_{load} \quad (3)$$

If $P_{Diff} = 0$, all the power produced by the main PV source is equal to the power required by the main load ($P_{MS} = P_{load}$). Therefore, the state of charge of the batteries remains constant (batteries at rest) neglecting their self-discharge. The switches S (between the electrolyser and the DC bus) and Sf (between the fuel cell and the DC bus) are in OFF state.

If $P_{Diff} > 0$, the power generated by the main source (PV) is greater than the load demand. Therefore, there is enough energy to power the load and store the excess.

If $P_{Diff} < 0$, the energy produced by the PV source is not enough to power the load. In this case, the batteries and the fuel cell intervene to provide the energy needed to cover the load demand.

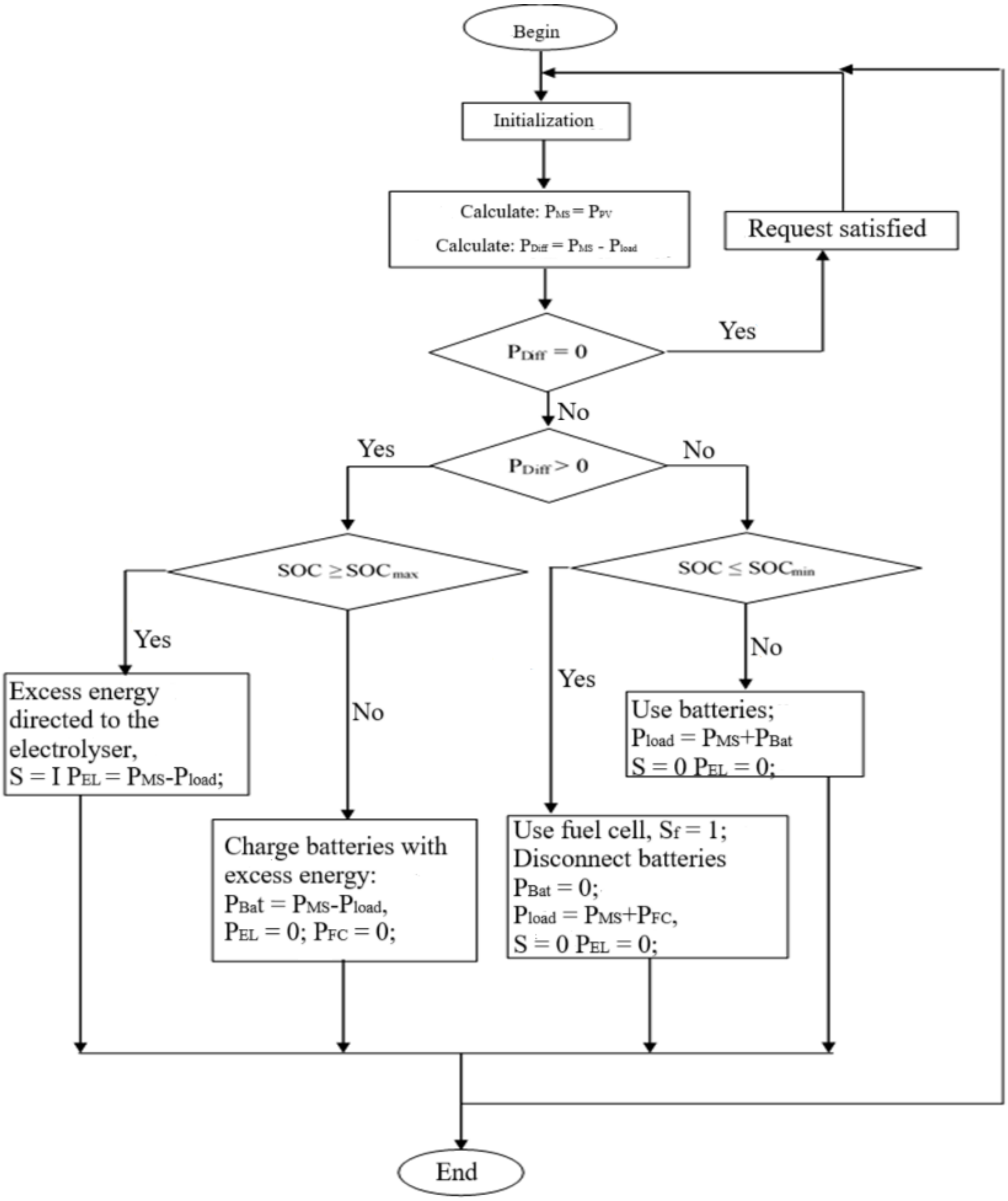

Fig. 2. Energy management flowchart of the hybrid power generation system

3.4 SIMULATOR INPUTS AND OUTPUTS

The input data required to simulate a year of operation are:

- The three annual profiles (Load profile, Sunshine profile, Ambient temperature profile);
- The component parameters.

The input profile for the load is an active power vector (in Watt peak) sampled in ten-minute time steps. An annual profile of global solar irradiation (in $Wh.m^{-2}$ and in the same ten-minute time step) is provided for sunshine. Many parameters must be entered before starting the simulation [29].

We can classify these parameters into characteristic parameters of the components (fixed) on the one hand, and on the other hand into component dimension parameters (adjusted during the dimensioning phases).

3.4.1 Load Profiles

Here, the load is of the individual housing type on an isolated site (autonomous over a year of operation).

Our approach is purely deterministic. The probable hazards at the load level (occasional consumption peaks) are not taken into account, the objective being the study of the proposed system according to the climatic conditions.

These synthesized annual load profiles start on January 1 of the year 2023 in Côte d'Ivoire (Yamoussoukro, INP-HB-Centre) and have a time step of ten minutes. Their construction is based on a sinusoidal function of time, whose phase shift and amplitude have a daily and seasonal variation.

All load profiles are defined by five parameters:

1. The annual average power (set at 1.72 kW);
2. The seasonal amplitude (10, 20, 30, 40 and 50% of the annual average power);
3. The seasonal phase shift (30 or 210 days, corresponding to higher consumption depending on the seasons of the year);
4. The daily amplitude (20, 40, 60 and 80% of the daily average power);
5. The daily phase shift (0, 4, 8 and 12 hours).

By combining these different amplitudes and phase shifts, we obtain one hundred and sixty (160 = 5× 2× 4× 4) load profiles that are generated, corresponding to one hundred and sixty different users. Figures 3 and 4 allow us to visualize the different amplitudes and phase shifts on the profiles.

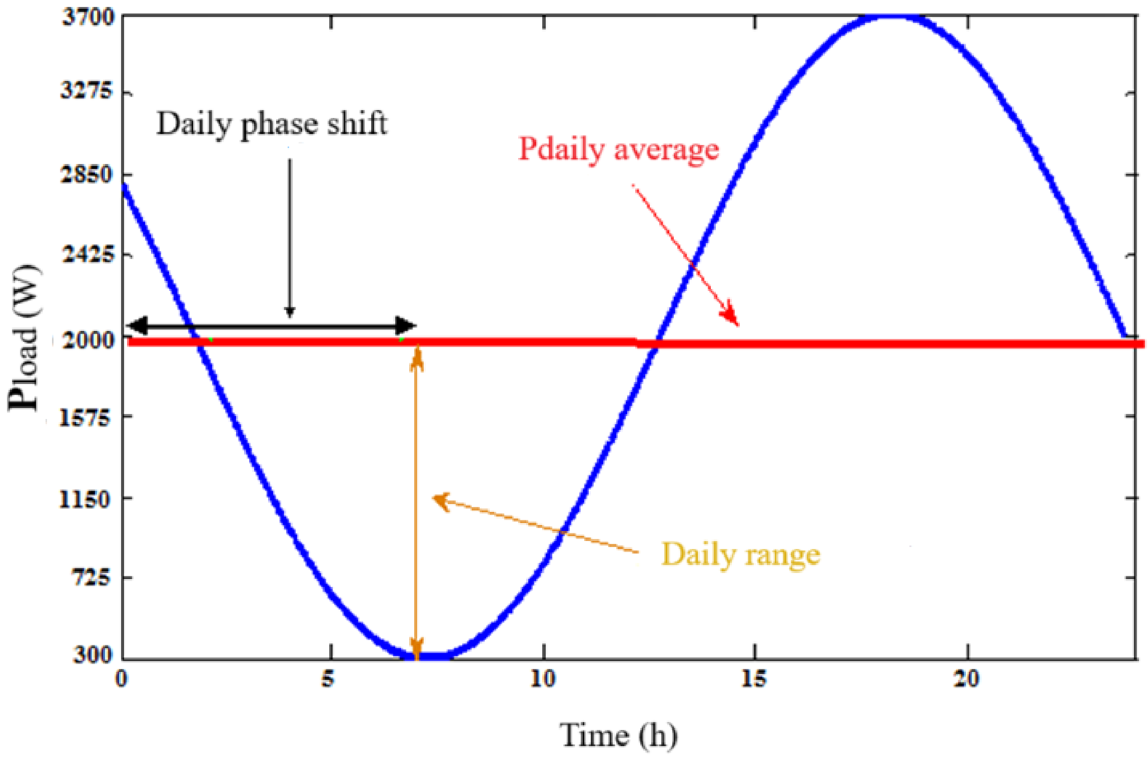

Fig. 3. Daily load profile (Daily variation in consumption)

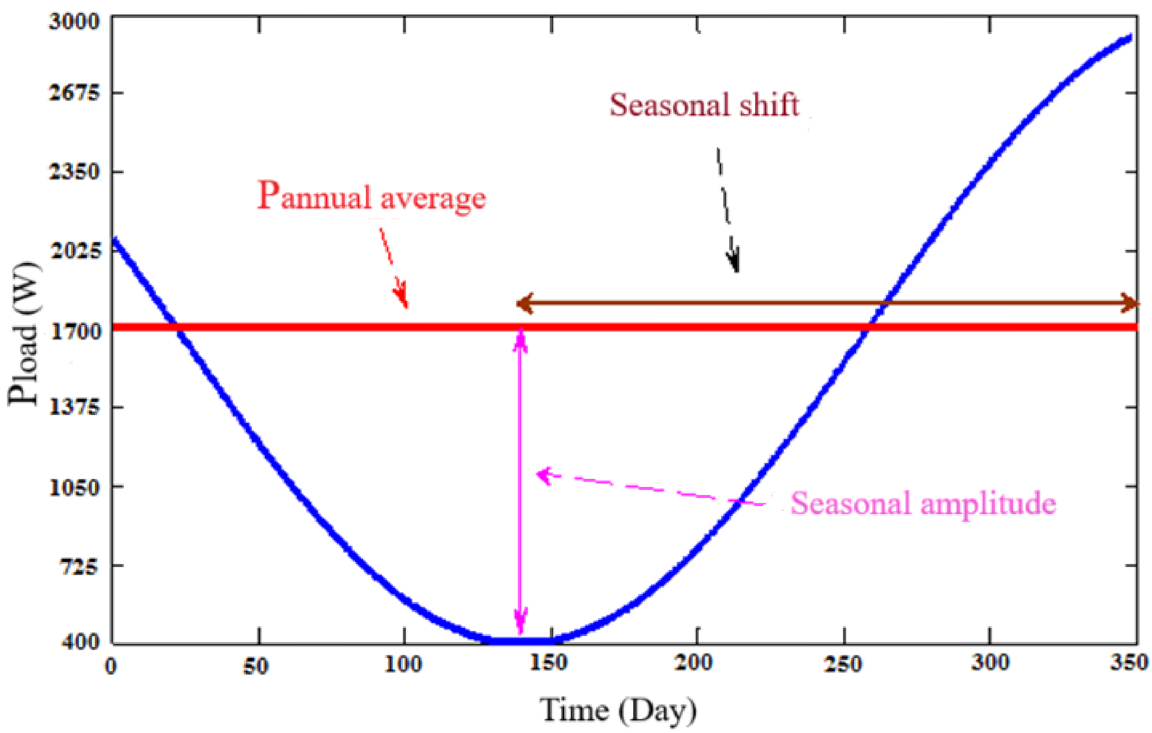

Fig. 4. Annual load profile (Annual variation of average daily power)

3.4.2 Sunshine Profiles

3.4.2.1 Sunshine Parameters

Installing a photovoltaic field involves defining several parameters beforehand, namely the inclination of the panels relative to the horizontal plane and the orientation of the panels relative to the cardinal points (azimuth).

The choice of the inclination and azimuth of the photovoltaic panels depends on the needs of the end user.

3.4.2.1.1 The Inclination Of The Panels

It allows, depending on the season, the adjustment of the captured solar energy. Thus, low inclinations maximize the production of the solar field over certain periods and high inclinations maximize production during other periods of the year in the northern hemisphere. For a given location and annual solar irradiation profile, an inclination can be determined that maximizes the capture of solar energy over the year. Figure 5 shows an example of variations in solar insolation as a function of the inclination of the solar field for January 1 of a typical year in Yamoussoukro (azimuth: due south). These data are theoretical and were taken from the PVGIS (Photovoltaic Geographical Information System) database.

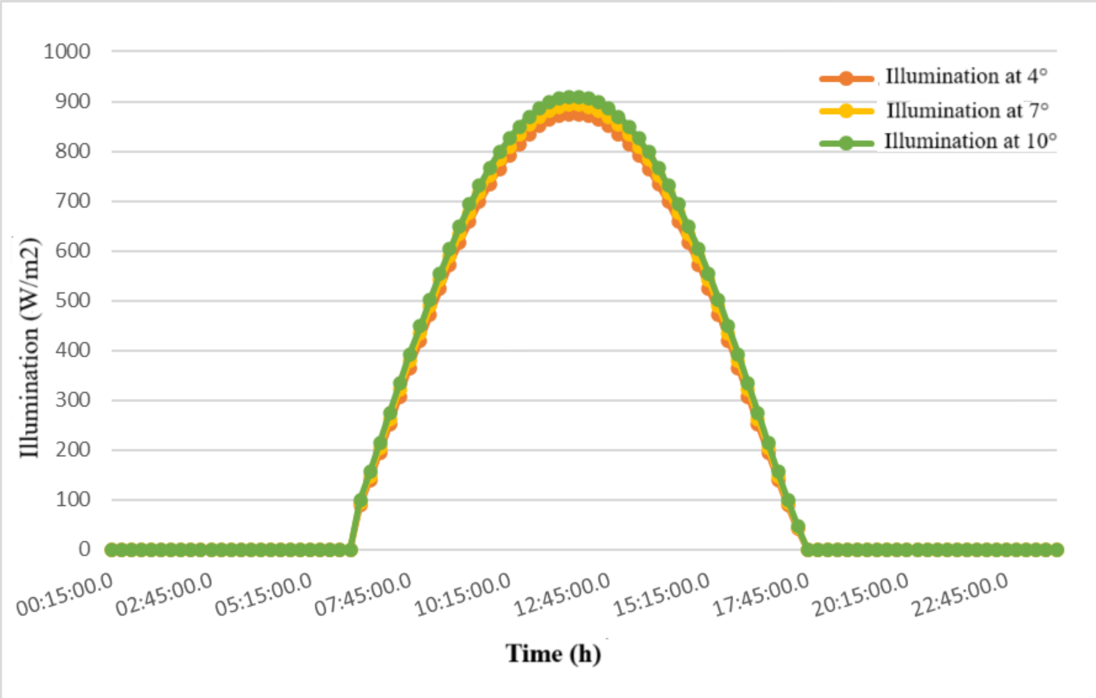

Fig. 5. ***variation of illumination according to the inclination of the photovoltaic solar panels, for the first day of January for a typical year at INP-HB-CENTRE [37; 38]***

Tableau 16. ***Available sunshine as a function of inclination; the month of January for a typical year at INP-HB-CENTRE [37; 28]***

Tilt	4°	7°	10°
Daily sunshine (Wh/m^2/j)	4243,67	4361,5	4464

The daily solar energy available for the same day, at the same location but for different inclinations, is presented in Table 16. It is clear that the available solar energy increases with the inclination of the panels.

3.4.2.1.2 Choice Of Panel Inclination

The inclination of the panels depends on the consumption profile of the end user and the storage system considered.

Regardless of the type of use, the panels are inclined so as to capture the maximum amount of energy during the year.

3.4.2.1.3 Azimuth

It allows the adjustment of the daily capture of solar energy. Maximum solar irradiation generally occurs at noon (sun at its zenith), therefore, a due south orientation (in the northern hemisphere) therefore allows the maximum collection of solar energy at the time when irradiation is at its maximum. By directly using the energy captured by the field, if the user's needs are greater in the morning, a south-east orientation of the panels will be preferred in order to capture as much as possible at this time of day [27; 29].

3.4.2.1.4 Choice Of Azimuth

The load profiles that we tested have different daily phase shifts. We could have adjusted the azimuth of the solar panels according to the value of the daily phase shift of the tested profile. The number of cases to be considered would have increased considerably.

In order to focus on the most relevant parameters and given that our study is located in the northern hemisphere, the azimuth was therefore deliberately set due south.

3.4.2.1.5 Sunshine Profiles

The sunshine profiles used come from the PVGIS database [39]. These are "typical" year profiles, synthesized from real measurements taken over several years.

The data collected with an hourly step are the overall sunshine (W/m^2) and the ambient temperature (°C). The data are then interpolated to generate profiles with a ten-minute time step.

The chosen geographical location is Yamoussoukro (INP-HB-CENTRE, Energy Engineering) whose coordinates are: 6°52’52” North Latitude, 5°13’47” West Longitude and the azimuth (due south).

There will therefore be two sunshine profiles in reality which correspond to the inclinations maximizing energy capture:

- Over the year (inclination 1),
- Over the most unfavorable period (inclination 2).

The following table 17 presents the information relating to the chosen location [37; 38].

Tableau 17. Coordinates of the chosen location and associated inclinations

Tilt	INP-HB-CENTRE
Coordinates	6°52'52" North Latitude, 5°13'47" West Longitude
Tilt 1	4°
Tilt 2	10°

4 Conclusion

The dimensioning allows to obtain a good overall operation and limits the cost of the installation. It allowed us to establish relationships between the powers of the components by simple rules, to define the solar power and the storage volume necessary to meet the demand of a load on a given site. The choice of electrochemical components is difficult because it is necessary to find the best compromise between efficiency, reliability and durability. Thus, the alkaline electrolyser seemed preferable to us for its efficiency and its lifespan. On the other hand, its peripheral must be optimized in terms of reliability and intrinsic consumption. The PEM technology fuel cell was chosen for its fast start-up time, its solid structure, its insensitivity to CO_2 and its compactness. A sensitivity study was carried out in order to determine the values of the torque (K_{el}, C_{nom}) allowing to obtain better simulation results. This study also made it possible to set up an electrical architecture and a control strategy capable of limiting conversion losses and optimizing energy management within the system.

References

[1] V. Khare, S. Nema, P. Baredar, «Solar–wind hybrid renewable energy system», a review. Renew Sustain Energy Rev; 58: 23–33, 2016.

[2] B. Boya Bi, P. Gbaha, « Sizing of an electric energy production hybrid system», Asian Journal of Science and Technology, Vol. 08, Issue, 11, pp.6669-6676, November, 2017.

[3] R. Belfkira, L. Zhang, G. Barakat, «Optimal sizing study of hybrid wind/PV/diesel power generation unit», Solar Energy 85 100–110, 2011.

[4] Y. Sawle, S. C. Gupta, A. K. Bohre, «Review of hybrid renewable energy systems with comparative analysis of off-grid hybrid system», Renewable and Sustainable Energy Reviews 81 2217–2235, 2018.

[5] M. Y. Masip, V. Javier, C. L. Ramirez, D. Wolfgang, « Assessment of on-site steady electricity generation from hybrid renewable energy systems in Chile», Applied Energy (Elsevier), Vol.250, pp.1548 – 1558, 2019.

[6] E. Omar, A. Abdulrahman, «Integrated Economic Adoption Model for residential grid-connected photovoltaic systems: An Australian case study», Energy Reports (Elsevier), Vol.5, 310 – 326, 2019.

[7] K. Ibrahim, S. Chindo, «Renewable energy consumption and economic growth nexus: A fresh evidence from West Africa», Energy Reports (Elsevier), Vol.5, pp. 384 – 392, 2019.

[8] Razmjoo, R. Shirmohammadi, A. Davarpanah, F. Pourfayaz, A. Aslani, «Stand-alone hybrid energy systems for remote area power generation», Energy Reports (Elsevier), Vol.5, pp.231 – 241, 2019.

[9] M. Child, C. Kemfert, D. Bogdanov, C. Breyer, «Flexible electricity generation, grid exchange, storage for the transition to a 100% renewable energy system in Europe», Renewable Energy (Elsevier), Vol.139, pp. 80 – 101, 2019.

[10] M. Hemeidaa, M. H. El-Ahmarb, A. M. El-Sayedc, H. M. Hasaniend, S. Alkhalafe, M. F. C. Esmaila, T. Senjyuf, «Optimum design of hybrid wind/PV energy system for remote area», Ain Shams Engineering Journal 11, 11–23, 2020.

[11] S. Sarangthem, F. Eugene, «Modeling size optimization and sensitivity analysis of a remote hybrid renewable energy system», Energy; 143: 719–31, 2018.

[12] K. Abla, B. S. Chokri, R. Djamila, M. M. Faouzi, «Sizing methodology for hybrid photovoltaic/wind/hydrogen/battery integrated to energy management strategy for pumping system», Energy; 153: 743–62, 2018.

[13] G. Narges, K. Alibakhsh, T. Ashkan, B. Leyli, M. Amin, «Optimization a hybrid wind-PV-battery system using GA-PSO and MOPSO for reducing cost and increasing reliability», Energy; 154: 581–91, 2018.

[14] A. Masud, «The application of Homer optimization software to investigate the prospects of hybrid renewable energy system in rural communities of Sokoto in Nigeria», Int J. Elec Comp Eng (IJECE); 7 (2): 596–603, 2017.

[15] M. Jayachandran, G. Ravi, «Design and optimization of hybrid micro-grid system», Energy Procedia; 117: 95–103, 2017.

[16] R. Dufo-Lopez, I. R. Cristóbal-Monreal, J. M. Yusta, «Stochastic-heuristic methodology for the optimization of components and control variables of PV-wind-diesel-battery stand-alone systems», Renewable Energy 99, 919-935, 2016.

[17] Askarzadeh, L. D. S. Coelho, «A novel framework for optimization of a grid independent hybrid renewable energy system: A case study of Iran», Solar Energy 112, 383–396, 2015.

[18] Alzgool, M., Khalaf, A.A., Nasan, O., Khatabi, L., Alrifai, M.A. (2023). Design and simulation of a renewable energy-based smart grid for Ma'an City, Jordan: A feasibility study. International Journal of Energy Production and Management, 8 (4): 219-227.https://doi.org/10.18280/ijepm.080403.

[19] L. Huang, «Research on optimal configuration of AC/DC hybrid system integrated with multiport solid-state transforms and renewable energy based on a coordinate strategy», Electrical Power and Energy Systems 119, 105880, 2020.

[20] S. Irtaza, «Near-optimal standalone hybrid PV/WE system sizing method», Sol Energy; 157: 727–34, 2017.

[21] Neffati, «Stratégies de gestion de l'énergie électrique d'un système multi-source: décision. Floue optimisée pour véhicule électrique hybride», Thèse de Doctorat, Université de Toulouse III Paul Sabatier, 2013.

[22] G. Koucoi, D. Yamegueu, Quoc-Tuan Tran, Y. Couliblay, H. Buttin, «Energy Management Strategies for Hybrid PV / Diesel Energy Systems: Simulation and Experimental Validation», Int J Energy Power Eng; 5: 6–14. doi: 10.11648/j.ijepe.20160501.12, 2016.

[23] G. Shen, J. Liu, H. Bin Wu, P. Xu, F. Liu, C. Tongsh, K. Jiao, J. Li, M. Liu, M. Cai, J. P. Lemmon, G. Soloveichik, H. Li, J. Zhu, Y. Lu, «Multi-functional anodes boost the transient power and durability of proton exchange membrane fuel cells», Nature Communications | 11: 1191.https://doi.org/10.1038/s41467-020-14822-y www.nature.com/naturecommunications, 2020.

[24] N.M. Sid, M. Becherif, K. Marouani, H. Alloui, «Gestion de l'énergie d'un système hybride pile à combustible/ batterie basée sur la commande optimale», Mediterranean Journal of Modeling and Simulation, Vol. 03, pp. 010 – 024, 2015.

[25] M. Nordio, F. Rizzi, G. Manzolini, M. Mulder, L. Raymakers, M. van S. Annaland, F. Gallucci and, « Experimental and modelling study of an electrochemical hydrogen compressor», Chemical Engineering Journal (Elsevier), Vol.369, pp. 432 – 442, 2019.

[26] M. A. Elhadidy, S. M. Shaahid, «Parametric study of hybrid (wind + solar + diesel) power generating systems», Renewable Energy, vol. 66 n 1, pp 129-139, 1999.

[27] J. Labbé, «l'Hydrogène électrolytique comme moyen de stockage d'électricité pour systèmes photovoltaïques isolés», Thèse de doctorat de l'Ecole des Mines de Paris, N° d'ordre: 1434, 2006.

[28] Boya Bi, K. B. Koua, P. Gbaha, E. P. M. Koffi, «Etude d'un système hybride de production d'énergie», Afrique SCIENCE, vol.16 n°5, pp 203 – 217, 2020.

[29] Bati Ernest Boya Bi, « Etude et Modélisation d'un système hybride (Piles à combustible-panneaux solaires photovoltaïques) pour la couverture totale en énergie électrique d'un site isolé en zone rurale», Thèse de doctorat de l'Institut National Polytechnique Houphouët Boigny (INP-HB) de Yamoussoukro: 2020.

[30] Ma, T., Li, M., Kazemian, A. (2020). Photovoltaic thermal module and solar thermal collector connected in series to produce electricity and high-grade heat simultaneously. Applied Energy, 261: 114380. https://doi.org/10.1016/j.apenergy.2019.114380.

[31] Rahimi, M., Azimi, N., Nouira, M., Shahsavar, A. (2023). Experimental study on photovoltaic panels integrated with metal matrix sheets and bio-based phase change materials. Energy, 262: 125371. https://doi.org/10.1016/j.energy.2022.125371.

[32] Ventura, C., Tina, G.M., Gagliano, A., Aneli, S. (2021). Enhanced models for the evaluation of electrical efficiency of PV/T modules. Solar Energy, 224: 531-544. https://doi.org/10.1016/j.solener.2021.06.018

[33] E. Ogliari, F. Grimaccia, S. Leva, M. Mussetta, «Hybrid Predictive Models for Accurate Forecasting in PV Systems», Energies, Vol.6, pp. 1918 – 1929, 2013.

[34] H. Shayeghi, Y. Hashemi, «Potentiometric of the Renewable Hybrid System for Electrification of Gorgor Station», Journal of Operation and Automation in Power Engineering Vol. 8, No. 1, Pages: 1-14, Feb. 2020.

[35] J. Li, S. Wang, L. Ye, J. Fang, «A coordinated dispatch method with pumped-storage and battery-storage for compensating the variation of wind power», Protection and Control of Modern Power Systems 3: 2 DOI 10.1186/s41601-017-0074-9, 2018.
[36] X. Li, L. Yao, D. Hui, «Optimal control and management of a large-scale battery energy storage system to mitigate fluctuation and intermittence of renewable generations», State Grid (Springer), Vol.4, n°4, pp. 593 – 603, 2016.
[37] http://re.jrc.ec.europa.eu/pvgis/apps4/pvest.php?map=africa&lang=fr, Mai 2017.
[38] K. N'tsoukpoe, « Effet des angles d'inclinaison et d'orientation des capteurs solaires sur leur production: cas des capitales des pays d'Afrique de l'Ouest et du Centre», Laboratoire Énergie Solaire et Économie d'Énergie (LESEE), Institut International de l'Ingénierie de l'Eau et de l'Environnement, Avril 2017.
[39] F. Laurencelle, R. Chahine, J. Hamelin, K. Agbossou, M. Fournier, T. K. Bose, «Characterisation of Ballard MK-E Proton exchange membrane fuel cell stack», Fuel Cell from fundamentals to systems 2001, n°1, pp. 66-71, 2001.